

Fig. 1. Diffuse reflection photograph of vanadium. On the left-hand side is a strong Laue spot. To the right of this is the diffuse 110 reflection. Above and to the right is a small spot due to an extra structural diffuse reflection.

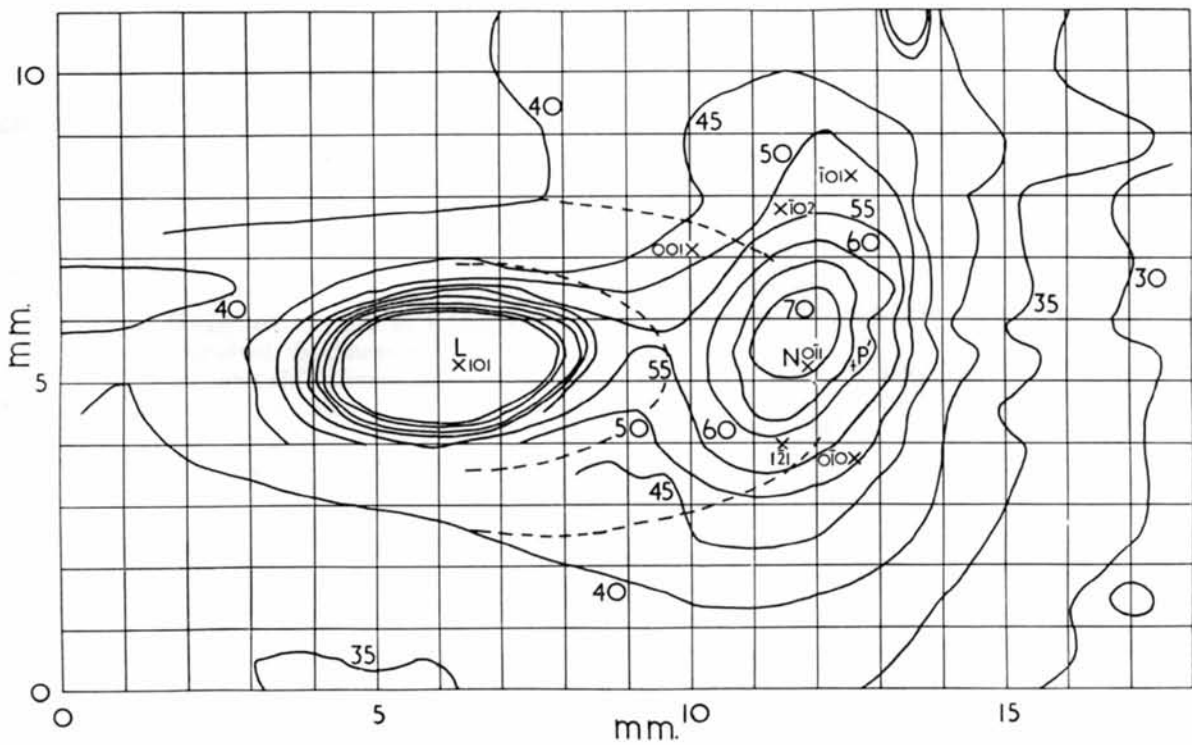


Fig. 2. Microdensitometer contour diagram. The figures are scale divisions on the recorder chart. The dotted lines indicate extrapolated background density surrounding the Laue spot.

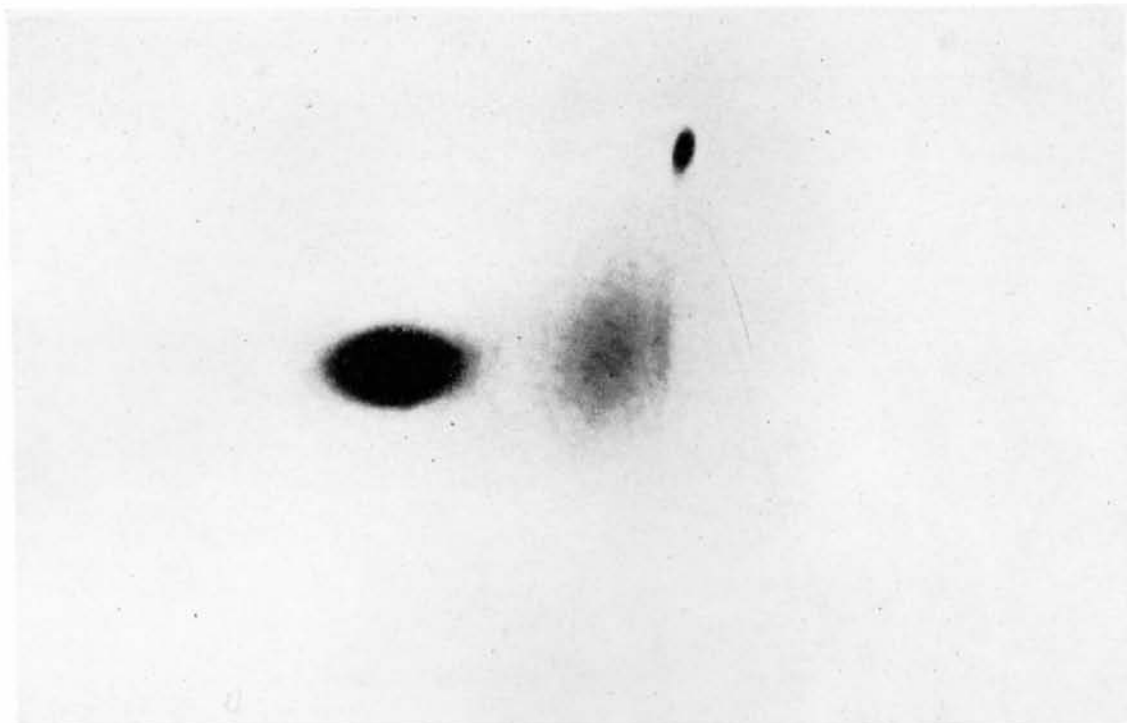


Fig. 1. Diffuse reflection photograph of vanadium. On the left-hand side is a strong Laue spot. To the right of this is the diffuse 110 reflection. Above and to the right is a small spot due to an extra structural diffuse reflection.

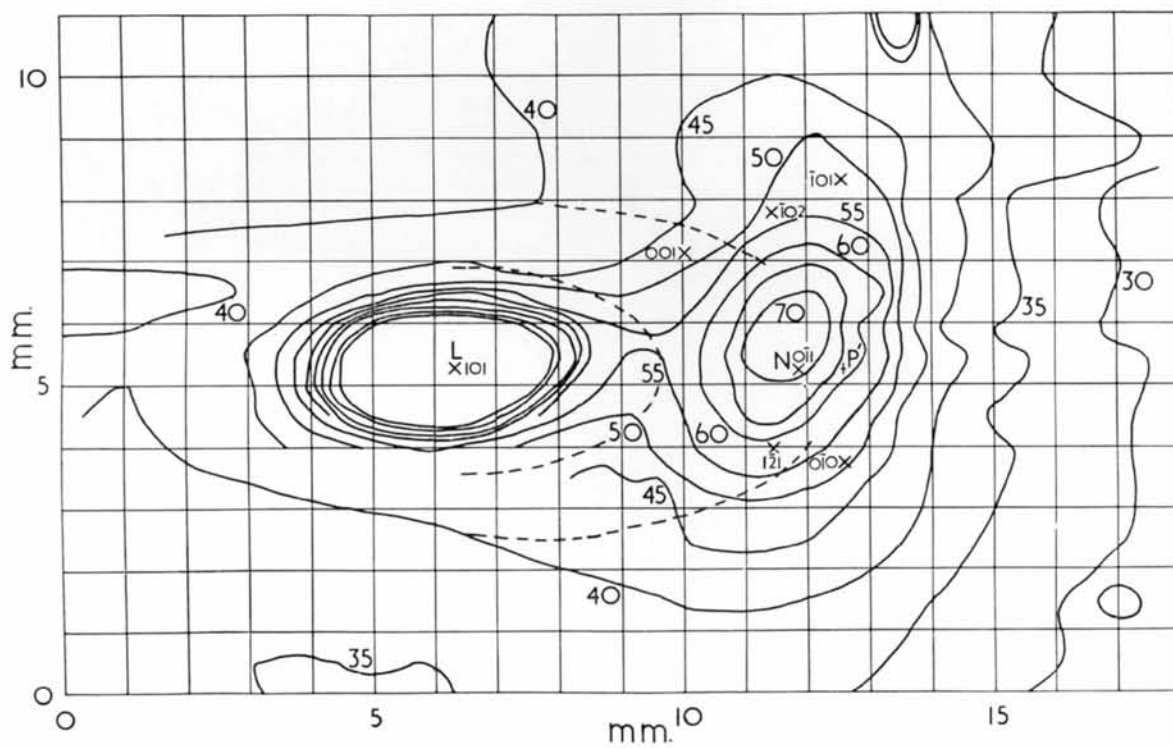


Fig. 2. Microdensitometer contour diagram. The figures are scale divisions on the recorder chart. The dotted lines indicate extrapolated background density surrounding the Laue spot.

Table 1. *Data on the diffuse reflection from vanadium*

rekha	Intensity			$K_0^* = 5.35$ cm.	K^* $(K_0^*/K^*)^2$	Skew corr.	Diverg. corr.	D_1
	Peak	Back- ground	Diff.					
$\bar{1}01$	51	37.5	13.5	10.30	0.29	1.163	1.00	54
$\bar{1}02$	52	40.2	11.8	8.99	0.38	1.126	1.00	35
001	48	42.2	5.8	9.00	0.38	1.085	1.00	16.5
$0\bar{1}0$	51	38.8	12.2	7.12	0.61	1.163	1.00	23.5
$1\bar{2}1$	58	41	17	6.68	0.69	1.126	0.98	27

important point in Fig. 2 is the foot of the perpendicular, N , from the relp (Ramachandran & Wooster, 1951) on to the film. There are several ways in which this may be found. The value of $(i-\theta)$ determines the distance of N from the centre of the Laue spot. The angle $(i-\theta)$ was determined by a photograph in which the Laue and Bragg spots were recorded as small well defined spots. The corresponding value of the ratio, s , of the distance PN to the radius of the reflecting sphere, is 0.0352. On Fig. 2 the Bragg spot is represented by P' and the Laue spot by L . A second method of fixing the position of N was afforded by the extra reflections. A careful study had been made of the φ -values corresponding to these reflections and the angle corresponding to the extra line just to the right of the diffuse spot in Fig. 1 was known. From this also the positions of the Bragg reflection P' , the Laue spot L , and N could be found. A third check was provided by the Kossel lines present on the film. These are due to the $V K\alpha$ radiation generated on the crystal and their intersections fix certain directions relative to the crystallographic axes.

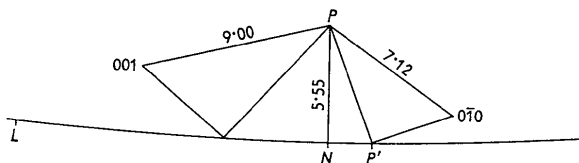


Fig. 3. Diagram showing geometrical construction by which the q -, φ -values of rekhas are transferred to Fig. 2.

A graphical method was used for determining the points of emergence of the rekhas (Ramachandran & Wooster, 1951) indicated in Fig. 2. The diagram used for this interpretation is shown in Fig. 3. The q -, φ -values (Hoerni & Wooster, 1952) were calculated from the known orientation of the crystal and by means of Fig. 3 these angles were converted into rectangular coordinates in the microdensitometer diagram.

The data read off from Figs. 2 and 3 are given in Table 1. The intensity is given in arbitrary units. The radius of the reflecting sphere was made 157.8 cm. so that the microdensitometer diagram was on the same scale as the reflecting sphere. Using this magnification 1 mm. on the film corresponds to 27.2 mm. on the microdensitometer diagram. The millimetre divi-

sions on the film are shown in Fig. 2. The skew correction (Ramachandran & Wooster, 1951) is determined simply by the angles i and φ read off from Fig. 2. The divergence correction was found by superposing on the point in Fig. 2, corresponding to a given rekha, a grid of nine contiguous equal rectangles, the total area of the grid being the same as that of the Bragg spot, when exposed to the same density as the diffuse spot. The intensity at the centre of each of these nine areas was read off and the average found. Generally this was the same as the intensity at the point at the centre of the network. Where there was a difference the ratio was taken as the divergence correction. In view of the other inevitable inaccuracies and the smallness of the correction, the second-order diffuse reflection was not subtracted from the observed diffuse reflection.

Interpretation

Vanadium has three independent elastic constants c_{11} , c_{12} , and c_{44} , and from our experimental results we can obtain two ratios, namely, c_{12}/c_{11} , c_{44}/c_{11} which will be denoted χ_{12} and χ_{44} . Though in principle the χ -values can be directly derived from the rekhas with simplest indices, in this investigation it was found better to use all the rekhas and a least-squares procedure. This procedure was as follows. Particular values for χ_{12} and χ_{44} are assumed and the usual formulae (Ramachandran & Wooster, 1951) are applied to calculate the $c_{11}K[ABC]_{hkl}$ values, which are proportional to the experimentally determined D_1 values. The five ratios of $10c_{11}K[ABC]_{hkl}/D_1$ are calculated and the relative standard deviation of these ratios from their mean found. This relative standard deviation is taken as an index of the correctness of the choice of values of χ_{12} and χ_{44} . Ideally it should be zero, when a correct choice had been made. In fact, it only approaches zero in the manner shown in Fig. 4. The axis of the ordinates is χ_{12} and that of abscissae is χ_{44} . It will be seen that the contours of the minimum values for the relative standard deviation of all five ratios cover a narrow area centred about the point

$$\chi_{12} = 0.68, \quad \chi_{44} = 0.35. \quad (1)$$

Polycrystalline elastic constants

The elastic constants of the polycrystalline material can be calculated from the elastic constants of the

single crystal, and these formulae provide a check on the values determined above. Two approaches to the problem have been made by Voigt (1910) and Reuss (1929) respectively. Using superscripts to distinguish the formulae of these authors, the polycrystalline Young's modulus and rigidity modulus may be written in terms of the elastic constants or moduli,

$$E^V = \frac{(c_{11} - c_{12} + 3c_{44})(c_{11} + 2c_{12})}{2c_{11} + 3c_{12} + c_{44}}, \quad G^V = \frac{c_{11} - c_{12} + 3c_{44}}{5}. \quad (2)$$

$$E^R = \frac{5}{3s_{11} + 2s_{12} + s_{44}}, \quad G^R = \frac{5}{4s_{11} - 4s_{12} + 3s_{44}}. \quad (3)$$

In terms of the elastic ratios and the cubic compressibility β , these expressions may be rewritten:

$$E^V = \frac{3(1 - \chi_{12} + 3\chi_{44})}{\beta(2 + 3\chi_{12} + \chi_{44})}, \quad G^V = \frac{3(1 - \chi_{12} + 3\chi_{44})}{5\beta(1 + 2\chi_{12})}, \quad (4)$$

$$E^R = \frac{15\chi_{44}(1 - \chi_{12})}{\beta(1 + \chi_{12} + 3\chi_{44} + \chi_{12}\chi_{44} - 2\chi_{12}^2)}, \quad G^R = \frac{15\chi_{44}(1 - \chi_{12})}{\beta(3 + 3\chi_{12} + 4\chi_{44} + 8\chi_{12}\chi_{44} - 6\chi_{12}^2)}. \quad (5)$$

Table 2 shows the values of β given by Bridgman (1927, 1952) and the values extrapolated by the present authors to 200 °C.

Table 2. Values of the compressibility β

	30 °C. (cm. ² /kg.)	75 °C. (cm. ² /kg.)	200 °C. (cm. ² /dyne)
1927	6.09×10^{-7}	6.12×10^{-7}	
1952	6.19	6.22	
Extrapolated			6.43×10^{-13}

Hill (1952) has shown that the Voigt and Reuss expressions give results which diverge from the true values in opposite senses. For a series of combinations of χ_{12} , χ_{44} the corresponding values of E^V , G^V , E^R and G^R have been calculated. These calculated values are compared with the experimentally measured values which are as follows (in units of 10^{11} dyne/cm.²):

$$E = 12.4\text{--}13.1 \text{ (Hample, 1954); } 12.7 \text{ (Lacy \& Beck, 1956); } 13.6 \text{ (Rostoker, Yamamoto \& Riley, 1956); } 13.7 \text{ (Graft, 1956).}$$

$$G = 4.64 \text{ (Lacy \& Beck, 1956).} \quad (6)$$

The dotted lines in Fig. 4 show the values of the elastic ratios for which the formulae (4) and (5) give polycrystalline constants which are in the range of the experimentally determined values given above. As χ_{12} , χ_{44} are changed to correspond to a point at the centre of the area between the dotted lines, the values calculated for E^V , G^V and E^R , G^R respectively diverge from the observed values in opposite directions. The

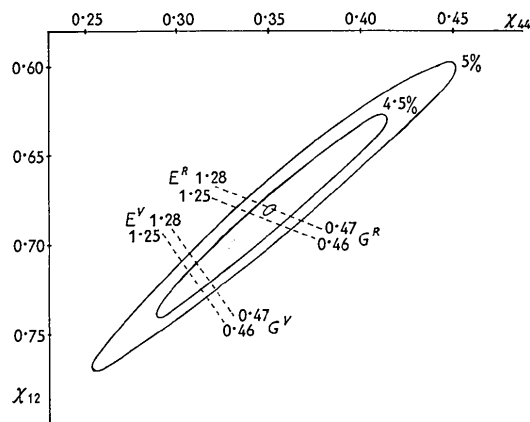


Fig. 4. The two full-line contours correspond to points in which the relative standard deviation of the five $10c_{11}K[ABC]_{hkl}/D_1$ ratios from their mean is 4.5% and 5% respectively. The dotted lines show the values of the elastic ratios for which the formulae (4) and (5) give polycrystalline elastic constants in the range of the experimentally determined E and G . (6).

true values of χ_{12} and χ_{44} must therefore lie in the area bounded by the two narrow strips.

Combining this evidence with the contours for the relative standard deviation of our five ratios we come to the conclusion that χ_{12} and χ_{44} must lie in the range

$$\chi_{12} = 0.70 \pm 0.02, \quad \chi_{44} = 0.33 \pm 0.02. \quad (7)$$

These values are in fair agreement with those derived from the thermal diffuse scattering measurements alone. We take as the true values of the elastic ratios the arithmetic means of (1) and (7), which gives

$$\chi_{12} = 0.69 \pm 0.02, \quad \chi_{44} = 0.34 \pm 0.02. \quad (8)$$

Note.—By combining the polycrystalline data with the thermal diffuse scattering measurements we ignored the fact that the polycrystalline elastic constants have been measured at room temperature, while our thermal diffuse scattering measurements refer to 200 °C. Nevertheless the temperature dependence of the polycrystalline elastic constants of metals suggests that the error arising in this way lies within the limits of accuracy of our measurements and thus it does not alter our results.

Absolute values of the elastic constants

The cubic compressibility is related to the elastic constants by the relation,

$$\beta = 3/\{c_{11}(1 + 2\chi_{12})\}.$$

As our measurements were made at 200 °C. the value of β due to Bridgman (1927, 1952) was extrapolated to this temperature and the value used was 6.43×10^{-13} cm.²/dyne. From the value for χ_{12} , namely 0.69, the value of c_{11} was determined. Finally from the elastic ratios the other two elastic constants were determined giving the final values

$$c_{11} = 19.6 \pm 0.3, \quad c_{12} = 13.5 \pm 0.2, \quad c_{44} = 6.7 \pm 0.5 \times 10^{11} \text{ dyne/cm.}^2.$$

We gratefully acknowledge the receipt of a grant from the Department of Scientific and Industrial Research in support of this work. We also wish to acknowledge the help afforded by the Brooklyn Crystallographic Laboratory, Cambridge in making a recording microdensitometer available to us.

References

- BRIDGMAN, P. W. (1927). *Proc. Amer. Acad.* **62**, 207.
 BRIDGMAN, P. W. (1952). *The physics of high pressure*. London: Bell.
 GRAFT, W. H. (1956). Unpublished measurements. Armour Research Foundation.
 HAMPLE, C. A. (1954). *Rare Metals Handbook*. Reinhold.
 HILL, R. (1952). *Proc. Phys. Soc. A*, **65**, 349.
 HOERNI, J. & WOOSTER, W. A. (1952). *Acta Cryst.* **5**, 626.
 LACY, C. E. & BECK, C. J. (1956). *Trans. Amer. Soc. Metals.* **48**, 579.
 RAMACHANDRAN, G. N. & WOOSTER, W. A. (1951). *Acta Cryst.* **4**, 431.
 REUSS, A. (1929). *Z. angew. Math. Mech.* **9**, 49.
 ROSTOKER, W., YAMAMOTO, A. S. & RILEY, R. E. (1956). *Trans. Amer. Soc. Metals.* **48**, 560.
 SALLER, H. A. & ROUGH, F. A. (1953). *Trans. Amer. Inst. Min. (Metall.) Engrs.* **197**, 545.
 SANDOR, E. & WOOSTER, W. A. (1958). *Nature, Lond.* **182**, 1435.
 VOIGT, W. (1910). *Lehrbuch der Kristallphysik*. Leipzig: Teubner.
 WOOSTER, W. A. (1955). *J. Sci. Instrum.* **32**, 457.

Acta Cryst. (1959). **12**, 336

An Optical Method for Producing Structure-Factor Graphs

BY C. A. TAYLOR AND F. A. UNDERWOOD

Physics Department, College of Science and Technology, Manchester 1, England

(Received 11 November 1958)

Structure-factor graphs (Bragg & Lipson, 1936) may be very informative at certain stages of a structure determination but the labour involved in their preparation is sometimes considered to be too great for profitable use. A simple extension of optical transform theory shows that they can be prepared easily and with sufficient accuracy for most purposes by the methods available for preparing optical transforms. Some examples are given, together with calculated graphs for comparison.

Introduction

In the course of a study of the projection on the basal plane of a hexagonal inorganic crystal transform methods were tried but were found to be of limited use. The projection under consideration has the probable two-dimensional space group $p6m$ and hence general positions of twelve-fold multiplicity. It is therefore difficult to consider first the transform of a single asymmetric unit and later the combined transform of all the related asymmetric units as suggested by Hanson, Lipson & Taylor (1953). The transform is, in fact, more obviously affected by the patterns produced by the symmetrical repetition of each atom than by the arrangement of the atoms within the asymmetric unit. This suggests that it may be better to consider the problem atom by atom rather than in terms of the whole asymmetric unit. Since the number of independent observable reflexions is small (nine for this structure) it seemed likely that structure-factor graphs (Bragg & Lipson, 1936) would provide a useful method of approach and attention was turned to the possibility of reducing labour by preparing them optically. The technique proves to be quite simple for this two-dimensional space group and

is applicable to all the other 16 groups, although for some it is a little more troublesome.

Use of structure-factor graphs

Structure-factor graphs are contoured maps showing the combined contribution of an atom and its symmetry-related counterparts to a particular reflexion as a function of the position of the atom in the unit cell. They are probably most useful in semi-quantitative work in the earlier stages of structure determinations and can give rapid indications of the general plausibility of an atomic arrangement in terms of the agreement with selected reflexions. At a later stage the direction of probable atomic movements may be deduced and a useful feature is the possibility of assessing the 'sensitivity' of various atomic positions; where the slope of the structure-factor graph is steep, small movements make significant changes in the total structure amplitude but atoms lying on plateau-like regions may be moved a considerable distance without affecting that particular reflexion. Since structure-factor graphs are rarely used when accurate quantitative measurements are needed it seems probable that